Available online at www.sciencedirect.com
ScienceDirect
Journal of Molecular Catalysis A: Chemical 269 (2007) 22–29
JOURNAL OF MOLECULAR CATALYSIS A: CHEMICAL
www.elsevier.com/locate/molcata

Synthesis, structural characterization, catalase-like function and epoxidation activity of a mononuclear manganese(II) complex

Luciana Rebelo Guilherme [a], Sueli Maria Drechsel [a,*], Felipe Tavares [a], Carlos Jorge da Cunha [a], Silvana Terezinha Castaman [a], Shirley Nakagaki [a], Ivo Vencato [b], Adailton J. Bortoluzzi [b]

[a] *Departamento de Química, Universidade Federal do Paraná, Centro Politécnico, Jardim das Américas, CP 19081, 81531-990, Curitiba, Brazil*
[b] *Departamento de Química, Universidade Federal de Santa Catarina, Campus Universitário, 88040-900 Florianópolis, Brazil*

Received 20 October 2006; received in revised form 28 December 2006; accepted 29 December 2006
Available online 9 January 2007

Abstract

In this work we have prepared a manganese(II) complex using the tridentate ligand *N*,*N*-bis(2-pyridylmethyl)amine (bpma). The manganese complex was characterized by elemental analysis, conductivity measurements and infrared, electronic (UV–vis) and EPR spectroscopic techniques. The analysis of the complex obtained has shown that the formula is $[Mn(bpma)_2](ClO_4)_2$ (**1**), which was confirmed by the X-ray structure. The structure shows two different conformers with pseudo-octahedral geometry. The synthesized manganese complex displays efficiency in disproportion reactions of hydrogen peroxide producing water and dioxygen in catalase-like activity. Compound **1** has shown a high reactivity with initial velocity for generation of dioxygen of 1.34×10^{-5} mol s^{-1} in the absence of heterocyclic base, and 4.46×10^{-5} mol s^{-1} in basic medium. Oxidation of cyclohexene by oxygen donor iodosylbenzene (PhIO), using the complex in homogeneous and heterogeneous media as catalyst, has also been investigated. In homogeneous catalysis it was observed that the major product was the epoxide. However, in heterogeneous media the reaction becomes more selective towards alcohol formation. Oxidation reactions using H_2O_2 as oxidant have shown low yields probably due the hydrogen peroxide decomposition promoted by complex **1**.

Keywords: Mn(II)complexes; Catalase-like function; H_2O_2 decomposition; Epoxidation

1. Introduction

Manganese is an essential trace element for the healthy existence of many bacteria, plants and for humankinds [1]. The chemistry of manganese has received considerable attention due to the fact that manganese is believed to be catalytically active in a variety of metalloenzymes [2]. In fact, many catalytic studies have been developed in recent years, where manganese complexes have been found to exhibit a diversity of catalytic oxidation reactions on organic substrates in organic solvents [3]. In these reactions the most important topics of catalysis research has been to find an efficient catalyst for the selective insertion of an oxygen atom into organic substrates [4]. In order to increase the selectivity these reactions have been performed by means of manganese complexes immobilized in microporous solids such as zeolite Y [5]. Manganese complexes with pyridine and (pyridylmethyl)amine ligands have been presented in the literature and used in oxidation catalysis and H_2O_2 decomposition. The dinuclear manganese compounds used by Feringa and co-workers [6,7] were able to catalyze the oxidation of several alkenes to the corresponding epoxides using H_2O_2 as oxidants. Also mononuclear Mn(II) complexes in homogeneous and heterogeneous media have been employed [8–10]. Nature has developed ways to counter the toxic effects of H_2O_2 by its disproportion to water and dioxygen. Heme enzymes that carry out this two-electron process are termed catalases [11]. Non-heme Mn-containing catalases (Mn-CAT), the so-called pseudocatalases, are known to be produced by various bacteria such as *Lactobacillus plantarum*, *Thermus thermophilus* and *Thermoleophilum album* [12]. Binuclear manganese complexes ($[Mn(II)_2(\mu\text{-}O_2CCH_3)_3L_2]^+$) with bis(pyridylmethyl)amine ligands were studied for their ability to disproportionate hydrogen peroxide [13,14]. Manganese is also an essential component

* Corresponding author. Tel.: +55 41 3361 3299; fax: +55 41 3361 3187.
E-mail address: sueli@quimica.ufpr.br (S.M. Drechsel).

1381-1169/$ – see front matter © 2007 Elsevier B.V. All rights reserved.
doi:10.1016/j.molcata.2006.12.044

of photosynthetic oxygen evolution, most likely participating as the oxidant of water [15]. We are presenting here the synthesis, structure and spectroscopic characterization of a manganese(II) complex $[Mn(II)(bpma)_2](ClO_4)_2$ (bpma = *N*,*N*-bis(2-pyridylmethyl)amine). The reactivity of the complex for H_2O_2 disproportionation, as a functional model for Mn-CAT, and the catalytic activity of the complex for the oxidation of cyclohexene by oxygen donor iodosylbenzene (PhIO) in homogeneous and heterogeneous media have also been investigated.

2. Experimental

All reagents were utilized without previous purification. The ligand *N*,*N*-bis(2-pyridylmethyl)amine (bpma) was synthesized according to a method described previously [16].

2.1. Synthesis of the Mn(II) complex

The complex $[Mn(bpma)_2](ClO_4)_2$ was prepared by means a methanol (2 mL)/ethanol (4 mL) solution of the ligand bpma (1.59 g, 8 mmol) adjusted to pH 7.9 by adding drops of NaOH solution (40%, w/v) solution, with an aqueous solution (2 mL) of $Mn(O_2CCH_3)_2{\cdot}4H_2O$ (0.98 g, 4 mmol). The resulting light brown solution was then stirred at room temperature for 1 h, after which an aqueous solution (2 mL) of sodium perchlorate (1.84 g, 12 mmol) was added. After 5 days two small light brown crystals had formed which were collected by filtration. After a week more amorphous solid has formed. Yield: 2.59 g, 70%. Anal. calculated for $MnC_{24}N_6O_{11}H_{32}Cl_2$: C, 40.81; H, 4.57; N, 11.90. Found for the amorphous solid: C, 40.29; H, 3.46; N, 10.87. UV–vis data in CH_3CN (λ_{max}, nm (ε, $mol^{-1}\,L\,cm^{-1}$)): 340 (1417), 364 (1028), 450 (396). IR (cm^{-1}) as KBr pellet (vs, very strong; s, strong; m, medium; w, weak): 3289 (vs) ν(N–H); 1606 (s), 1571 (w), 1488 (m), 1436 (s), ν(C=C) and ν(C=N), 1101 (vs), 1081 (s), ν(Cl–O); 767 (s), 622 (s) δ(C–H) of pyridine group. Λ_m (CH_3CN, 298 K) 249 S cm^{-2} mol^{-1} for complex 1:2.

2.2. Immobilization of the complex

The immobilized compound was prepared by the slow addition of solid Mn^{2+}Y zeolite (0.33 g, 4.2% Mn^{2+}) to a bpma (0.5 mmol) solution in toluene (37 mL)/methanol (3 mL), with stirring, followed by reflux for 48 h at 90 °C. The mixture was centrifuged and the resulting yellow solid was washed in Soxhlet for 6 h with CH_2Cl_2, and then with toluene for 10 h, to remove unreacted ligand. The washed yellow solid was dried at 50 °C. The preparation of solid Mn^{2+}Y zeolite, obtained from the exchange reaction between NaY zeolite and Mn^{2+}, was conducted as described in the literature [9].

2.3. Physical measurements

Electronic absorption spectra were recorded on a Hewlett-Parckard 8452A spectrometer. Infrared spectra were recorded on a BOMEM model Hartmann & Braun MB-series Michelson spectrometer. X-band EPR spectra were collected on a Bruker ESP300 spectrometer at 77 K. A Perkin-Elmer 2400 elemental analyzer was used to collect micro analytical data (C, H, N). A Shimadzu GC-14B gas chromatograph using a cromatopac C-R6A column was used to identifying oxidation products of catalysis.

Table 1
Selected crystal data and structure refinement for $[Mn(bpma)_2](ClO_4)_2$

Empirical formula	$C_{24}H_{26}Cl_2MnN_6O_8$
Formula weight	652.35
Temperature (K)	293(2)
Wavelength	0.71073
Crystal system	Monoclinic
Space group	*C*2/*c*
Unit cell dimensions (Å, °)	$a = 23.936(5)$
	$b = 9.064(2)$
	$c = 26.143(4)$
	$\beta = 91.25(3)$
V (Å^3)	5670.5(19)
Z	8
Calculated density (g/cm^3)	1.528
μ (Mo Kα) (mm^{-1})	0.712
F (0 0 0)	2680
Theta range for data collection (°)	2.52–25.00
Index ranges	$0 \le h \le 28$, $0 \le k \le 10$, $-31 \le l \le 31$
Reflections collected/unique	5098/4969 [$R_{int} = 0.0198$]
Refinement method	Full-matrix least-squares on F^2
Data/restraint/parameters	4969/0/372
Goodness-of-fit on F^2	1.058
Final R indices [$I > 2\,\sigma(I)$]	$R1 = 0.0576$, $wR2 = 0.1343$
R indices (all data)	$R1 = 0.1114$, $wR2 = 0.1817$
Largest diff. peak and hole (e Å^{-3})	0.655 and −0.871

2.4. X-ray crystallographic analysis

The crystallographic analysis of $[Mn(bpma)_2](ClO_4)_2$ was carried out at room temperature with a CAD-4 Enraf Nonius diffractometer using graphite monochromated Mo Kα radiation ($\lambda = 0.71073$ Å). Cell parameters were determined from 25 centered reflections and refined with SET4 instruction and the data collection were made using ω–2θ scan technique. Both procedures were done with CAD-4 Express software [17]. Absorption corrections carried out on the basis on the azimuthal scans of 7 appropriate reflections were also applied to the collected intensities with the PLATON program [18,19]. The structure was solved using direct methods with SIR-97 [20]. The structure was refined by full-matrix least-square procedures on F^2 using SHELXL-97 [21]. The program WINGX was used in the refinement and analysis of the crystal structure [22]. Another selected crystallographic information are summarized in Table 1. The images were prepared using Platon [23]. Crystallographic data for the structural analysis of $[Mn(bpma)_2](ClO_4)_2$ have been registered with the Cambridge Crystallographic Data Center, CCDC 622717. Copies of this information may be obtained free of charge from The Director, CCDC, 12, Union Road, Cambridge CB2 1EZ (fax: +44 1223 336 033 or e-mail: deposit@ccdc.cam.ac.uk or http://www.ccdc.cam.ac.uk).

2.5. Studies on catalase-like function

All reactions were carried out at 15 °C and the dioxygen evolution was measured volumetrically. Each experiment was

conducted by adding of 1 mL of hydrogen peroxide MeCN solution (concentration from 2 to 7 M) to 1 mL of 1 mM solution of the complex in a 10 mL flask sealed with a rubber septum. The reactor was connected to a graduated burette filled with water.

2.6. Epoxidation of cyclohexene

Epoxidation of cyclohexene was carried out in homogeneous and heterogeneous media. In the homogeneous solution a mixture of 1 mg of catalyst (1.5 μmol, $[Mn(bpma)_2](ClO_4)_2$), oxidant (iodosylbenzene) at various concentrations (0–150 μmol), 250 μL solvent (CH_3CN) and 1.5 mmol substrate (cyclohexene) were magnetically stirred in an ice bath for 2 h. After this period the reaction products were immediately analyzed by GC. The catalytic studies with heterogeneous catalyst were performed in a similar manner as described for homogeneous catalysis.

3. Results and discussion

3.1. Characterization of the complex

The IR spectrum of the complex has a well defined N–H stretching at 3289 cm^{-1}. Strong peaks in the 1081–1101 cm^{-1} range are assigned to ν(Cl–O) stretching of the perchlorate ion present as counter-ion. The molar conductivity of an acetonitrile solution of the complex confirms the formation of a 1:2 electrolyte. Based on this data and on elemental analysis the formula of the complex was formulated as $[Mn(bpma)_2](ClO_4)_2 \cdot 3H_2O$, a monomeric Mn(II) complex with two bpma ligands, and two ClO_4^- ions. The elemental analysis was performed on the amorphous portion of the obtained solid. The EPR spectrum of an DMF solution of complex **1** at 77 K has six lines centered at $g = 2$ with $A = 92$ G (supplementary material), characteristic of a Mn(II) center in octahedral geometry. The spectrum of the acetonitrile solution of complex **1** at room temperature has a large signal at $g = 2$ (Fig. 3) and in dichloromethane besides this signal additional signals were observed in $g = 3.3$ and $g = 5.4$ (supplementary material). The signal observed in MeCN and DCM solutions are broad, and the manganese hyperfine splitting is not resolved. The observation of low- and high-field transitions, and the absence of the fine-structure, are indicative of more distorted geometry [24]. The differences of the EPR spectra in different solvents may be indicative of the equilibrium among the two conformers observed in the crystalline structure.

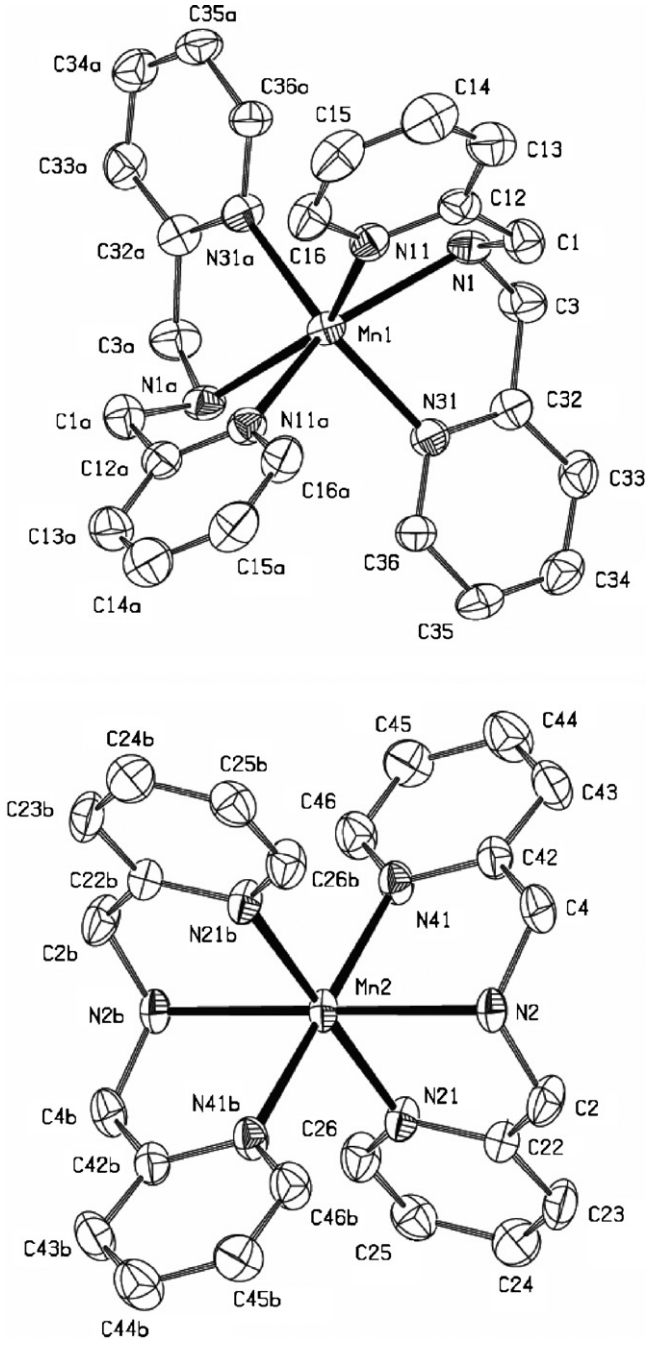

Fig. 1. ORTEP diagram of the two conformers of the cation complex $[Mn(bpma)]^{2+}$. Symmetry codes: (a) $-x+1, y, -z+1/2$; (b) $-x+3/2, -y+3/2, -z+1$.

3.2. X-ray structure

The ORTEP diagram of the complex cation is shown in Fig. 1. Selected bond distances and angles are shown in Table 2. The asymmetric unit presents two different conformers of $[Mn(bpma)_2]^{2+}$ with different local symmetry. In both conformers, the ligand bpma is facially coordinated to manganese ion. Conformer 1 (Mn1) has C_2 symmetry, where the secondary amine groups (N1 and N1a) and the pyridine groups (N11 and N11a) are *trans* to each other, being the equatorial plane defined by four N_{py} atoms. Conformer 2 (Mn2) shows a centrosymmetric structure with the two secondary amine groups (N2 and N2b) are coordinated in the axial positions (N2–Mn2–N2b 180°) and the atoms N21, N21b, N41 and N41b determine the equatorial plane. In both conformers, the Mn(II) ions are in distorted octahedral environment. However, the degree of the distortion is significantly different between them. Around Mn1, the *cis* angles vary from 72.78(16)° to 117.75(17)° and the average of *trans* angles is 143.45°, while around Mn2 the *cis* angles are ranging from 77.06(15)° to 102.94(15)° and the *trans* angles are 180° imposed by symmetry. Consequently, the bond lengths are smaller and close to each other in conformer 2 (average: equatorial 2.224 Å,

Table 2
Selected bond lengths (Å) and bonds angles (°) for $[Mn(bpma)_2](ClO_4)_2$

Bonds lengths (Å)		Bonds lengths (Å)	
Conformer 1 (Mn1)		Conformer 2 (Mn2)	
Mn1–N1	2.338(4)	Mn2–N2	2.275(4)
Mn1–N11	2.246(5)	Mn2–N21	2.222(4)
Mn1–N31	2.214(4)	Mn2–N41	2.227(4)
Angles (°)		**Angles (°)**	
Conformer 1 (Mn1)		Conformer 2 (Mn2)	
N31[a]–Mn1–N31	132.9(2)	N21–Mn2–N41	86.29(16)
N31–Mn1–N11[a]	96.62(16)	N21[b]–Mn2–N41	93.71(16)
N31–Mn1–N11	117.75(17)	N21–Mn2–N2	77.31(15)
N11[a]–Mn1–N11	86.8(2)	N41–Mn2–N2	77.06(15)
N31[a]–Mn1–N1	89.00(16)	N21–Mn2–N2[b]	102.69(15)
N31–Mn1–N1	72.78(16)	N41–Mn2–N2[b]	102.94(15)
N11[a]–Mn1–N1	148.73(16)	N2–Mn2–N2[b]	180.0(2)
N11–Mn1–N1	73.43(17)		
N1–Mn1–N1[a]	133.8(2)		

Symmetry codes: (a) $-x+1, y, -z+1/2$; (b) $-x+3/2, -y+3/2, -z+1$.

axial 2.275 Å) with respect to than those observed in conformer 1 (average: equatorial 2.230 Å, axial 2.338 Å).

3.3. Catalase-like activity

The reactivity of complex **1** towards hydrogen peroxide was investigated by measuring changes in UV–vis and EPR spectra, and by volumetric determination of evolved dioxygen. The catalytic activity of complex **1** was investigated in acetonitrile solutions in the presence and absence of imidazole (Fig. 2). The evolution of dioxygen promoted by the complex without base has shown an initial velocity of 1.3×10^{-5} mol s^{-1} of O_2, which indicates a conversion of 0.7×10^3 molecules s^{-1} of H_2O_2 per molecule of Mn, complex. The presence of imidazole enhances the initial rate to 4.5×10^{-5} mol s^{-1} (1.1×10^3 molecules H_2O_2 s^{-1} per molecule of Mn, complex). The crystal structure of the manganese catalase from *L. plantarum* reveals the presence of bases in the vicinity of the active site and it was proposed that they promote the transfer of the peroxidic protons during the turnover [24]. Despite the fact that complex **1** has a mononuclear structure, conversion rates are in the same range observed for a series of dinuclear manganese complexes [25–28]. However, these values are still much smaller than those observed for *L. plantarum* catalase (2×10^5 molecule s^{-1}), like seen for other Mn catalase mimics [29,30].

The EPR spectrum of the complex in CH_3CN solution at room temperature shows a large signal at $g = 2$ (Fig. 3a) characteristic of mononuclear Mn(II) complexes in a distorted octahedral symmetry [31]. After the addition of H_2O_2 the spectrum changes with enlargement of the signal at $g = 2$ and a hyperfine structure appears indicating the change of the initial geometry of the complex, and perhaps the oxidation state of the metal center, possibly promoted by the interaction with the H_2O_2 molecule. After 5 min a new signal at $g = 4$ appears (Fig. 3c) and a signal at $g = 2$ shows a

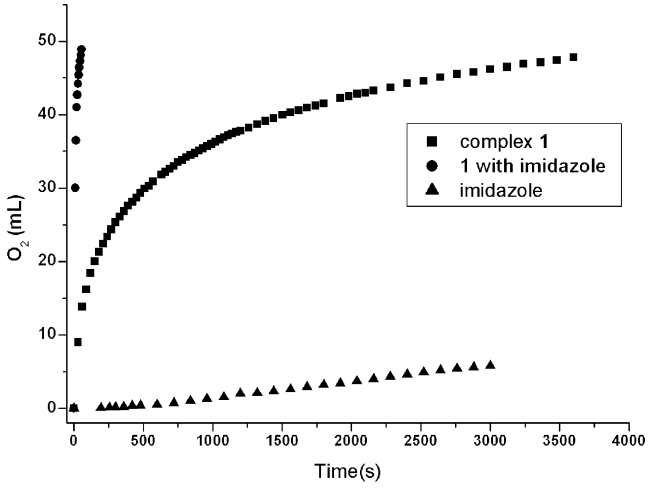

Fig. 2. Time-course profiles of dioxygen evolution (mL) from the reaction of H_2O_2 (1 mL, 30%) with: (■) complex **1** (1.0×10^{-3} mol/L), (●) complex **1** (1.0×10^{-3} mol/L) with imidazole (1.0×10^{-3} mol/L), (▲) just imidazole (1.0×10^{-3} mol/L) in acetonitrile solutions at 15 °C.

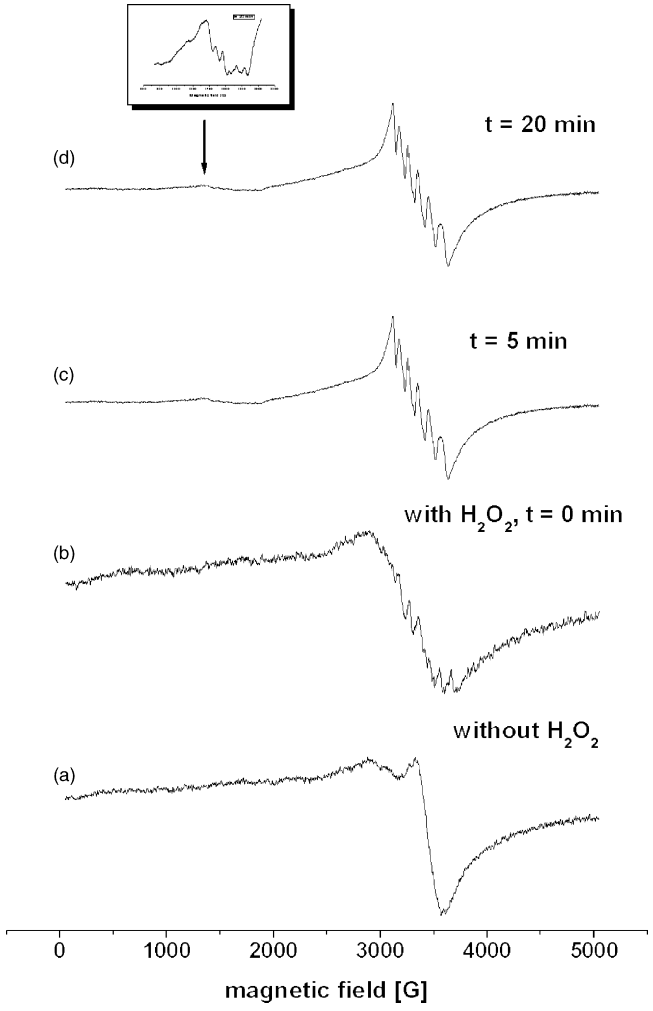

Fig. 3. X-band EPR spectra of complex **1** at room temperature and CH_3CN. Solution: (a) complex **1** solution (1.0×10^{-3} mol/L), (b) a few seconds after the addition of H_2O_2 (1 mL, 30%), (c) 5 min after addition of H_2O_2 and (d) 20 min after addition of H_2O_2 (ca. 9.5 GHz).

six line splitting typical of octahedral manganese(II) complexes (Fig. 3d).

Selected UV–vis spectra, obtained during the monitoring of the reaction between complex **1** and hydrogen peroxide, can be seen in Fig. 4. The addition of H_2O_2 to the complex solution promoted an absorbance increase in the 350–500 nm range, typical of metal center oxidation. After 4 min the absorbance decreases forming a new profile different from the initial observed for complex **1**. The solution spectra, recorded after 20 min of hydrogen peroxide addition, did not show appreciable differences indicating that a stable species was produced and that the original complex was not regenerated.

Based on EPR and UV–vis spectroscopic changes upon addition of H_2O_2 to complex **1** solutions, we propose two interaction mechanisms. It is known that the heterocyclic base accelerates the homolysis of the O–O bond and stabilizes a Mn(IV)=O intermediate species [32]. Considering this and the fact that the peroxide disproportionation involves a four-electron transferring process, the first mechanism proposed, Scheme 1, assumes that the mononuclear Mn(II) complex oxidation produces a Mn(IV) intermediate complex which produce the absorbance increase observed in the UV–vis spectra.

The second mechanism (Scheme 2), is similar to that proposed by Naruta and co-workers for manganese(III) porphyrins, that assumes a diporphyrinato dimanganese(III) intermediate

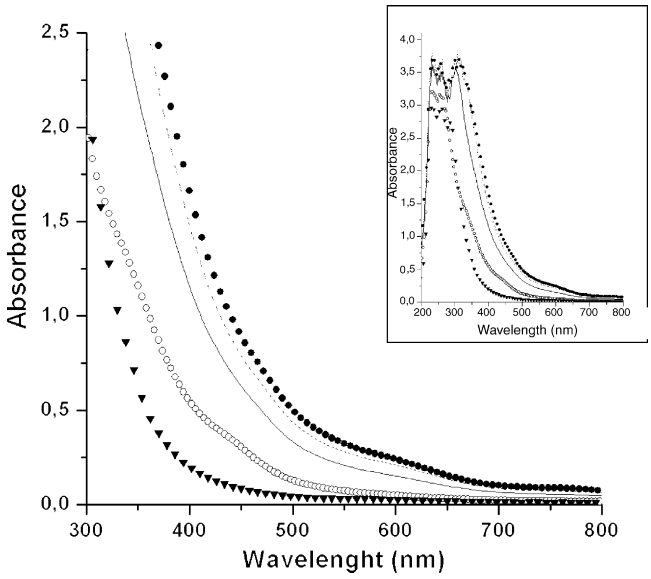

Fig. 4. Electronic spectra of complex **1** (1.0×10^{-3}) in acetonitrile with addition of H_2O_2 (50 μL, 30% solution): without H_2O_2 (◯); 30 s after addition of H_2O_2 (—); 1 min after addition of H_2O_2 (●); 4 min after addition of H_2O_2 (· · · ·) and 20 min after addition of H_2O_2 (▼).

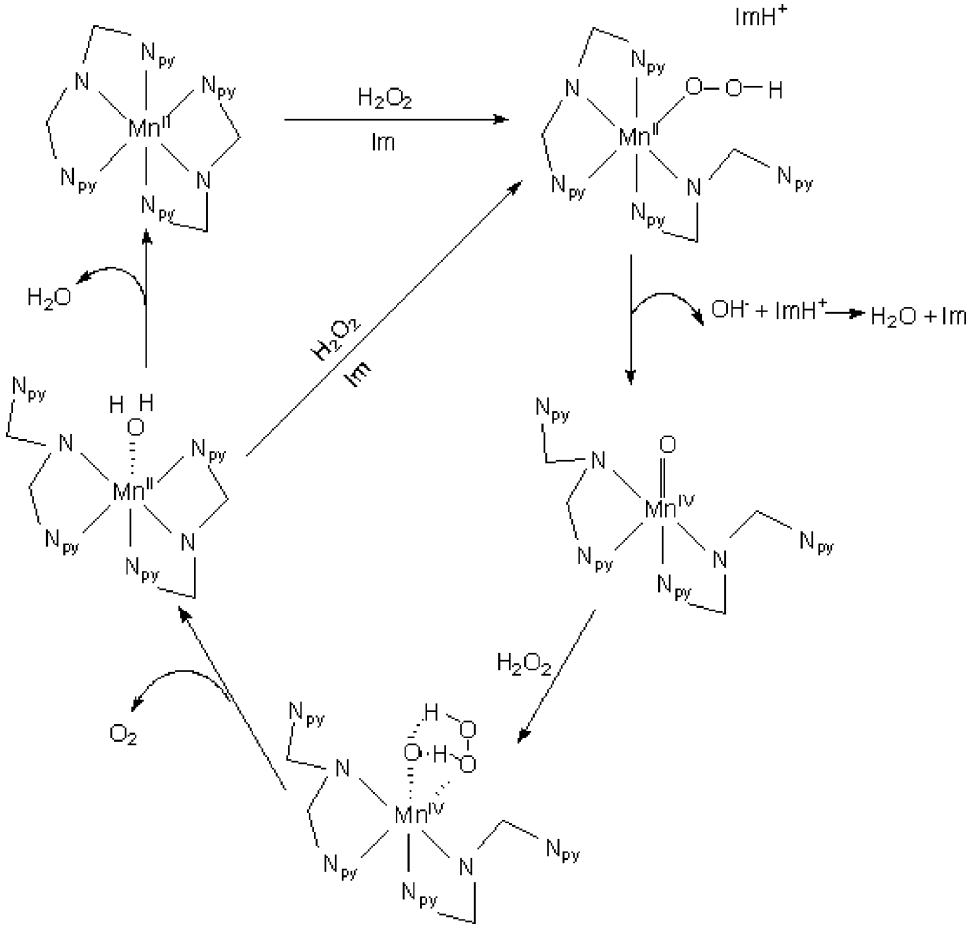

Scheme 1. .

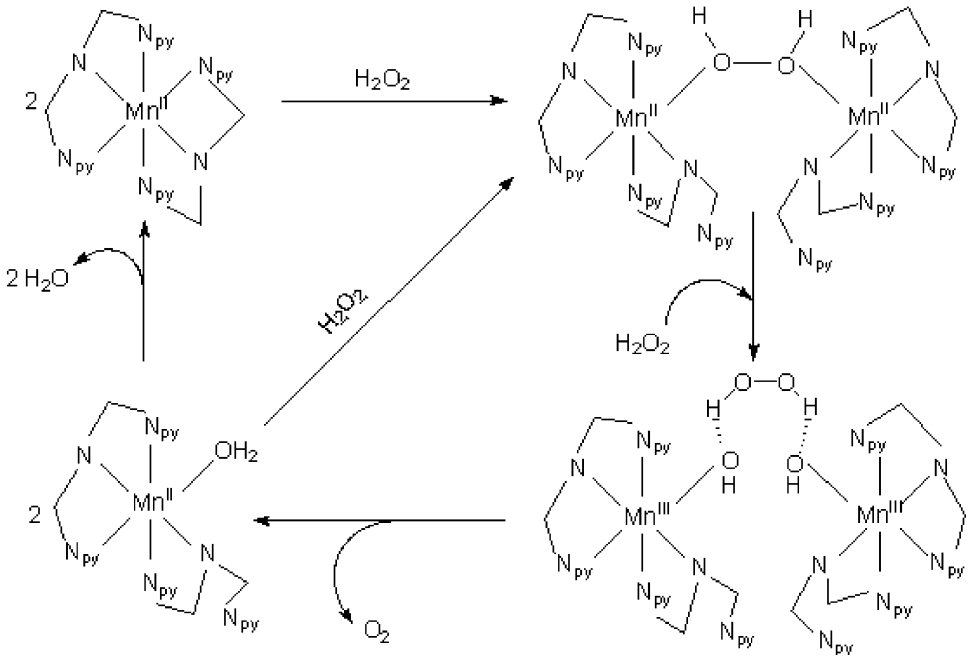

Scheme 2. .

Table 3
Epoxidation of cyclohexene catalyzed by $[Mn(bpma)_2](ClO_4)_2$ (homogeneous reaction) and MnYbpma (heterogeneous reaction)

Catalyst	Time (h)	Proportion (mol)	Conversion (%)[a]		
			Epoxide	Ketone	Alcohol
Complex **1**	2	100o:1000s	~0	~0	~0
		1c:100o:1000s	93	~0	~0
		1c:50o:1000s	68	6	~0
		1c:25o:1000s	67	~0	~0
MnYbpma	40	100o:1000s	1	0	3
		1c:100o:1000s	8	0	6
		1c:50o:1000s	12	5	43
		1c:25o:1000s	9	10	73

Legend: c: catalyst, o: oxidante, s: substrate.
[a] Based on oxidant concentration.

complex [32,33]. This mechanism which involves oxidized species bridged by hydroxide ions, was similar to that proposed to manganese diporphyrins linked by rigid structures such as anthracene. The binuclear Mn(III)Mn(III) structure would not be detected by EPR and would promote an absorbance increase. However, the improvement promoted by the imidazol base could not be easily demonstrated in this mechanism. More experimental studies are in course to better understand the operating mechanism.

3.4. Epoxidation of cyclohexene

The results of epoxidation of cyclohexene catalyzed by complex **1** in homogeneous medium and by the complex immobilized in zeolite (MnYbpma) with PhIO as oxidant, are shown

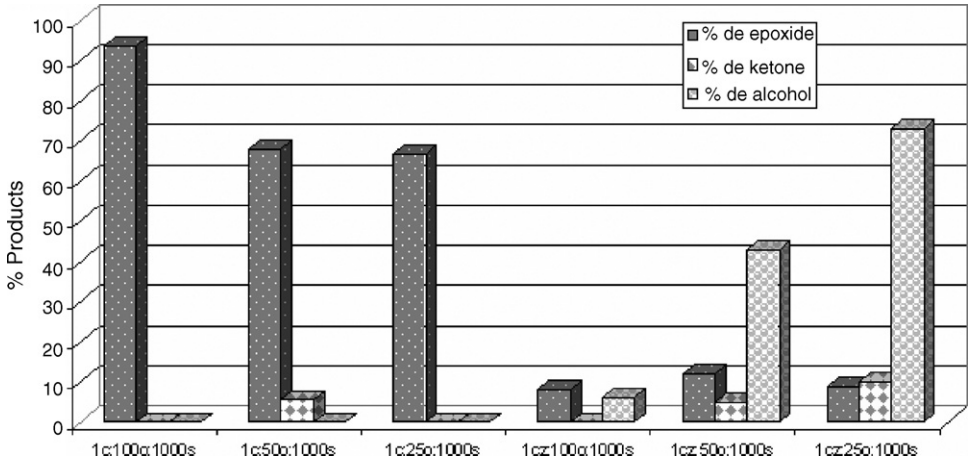

Fig. 5. Epoxidation of cyclohexene with (c) $[Mn(bpma)_2](ClO_4)_2$ and (cz) MnYbpma. Legend: c = catalyst, o = oxidante, s = substrate.

in Table 3 and in Fig. 5. The values found for conversion of cyclohexene with $[Mn^{II}(bpma)_2](ClO_4)_2]$ in homogeneous reaction have revealed more selective conversion for epoxide. Conversion rates observed for homogeneous reactions are similar to those observed for some metal porphyrins [34–36] and better then those observed for some other mononuclear Mn(II) complexes [37–39]. However, the heterogeneous catalyst gives now mainly alcohol as product. The formation of allylic products is generally attributed to a radical mechanism, promoted or not by the metal center, or generated by the presence of dioxygen. The role of the intermediate Mn specie as a radical initiator has been proposed to occur via activation of an allylic C–H bond [36,40,41]. The presence of included dioxygen inside the zeolite may be responsible for the preference of the radical mechanism observed in this work. In control experiments, without the complex in homogeneous medium, or with the zeolite with Mn(II) ions (without the ligand), epoxidation did not occur. The reaction of the Mn(II) zeolite with the oxidant promoted a color change of the solid from white to black probably due to formation of manganese oxide. This phenomenon was not observed when MnYbpma zeolite was used demonstrating that the bpma complexation protected the metal center. Low yields of cyclohexene epoxidaton were obtained when hydrogen peroxide was used as oxidant in homogeneous and heterogeneous media. These low conversion rates are attributed to the competitive parallel reaction of hydrogen peroxide decomposition promoted by complex **1** in homogeneous media, and also by the supported system.

4. Conclusions

The complex $[Mn(bpma)_2](ClO_4)_2$ was synthesized and structurally characterized by single-crystal X-ray diffractometry. Spectroscopic (UV–vis, EPR and IR) properties, in agreement with crystallographic results, confirmed that a mononuclear cation molecule with two ligand molecules and two perchlorates as counter-ions were obtained. The analysis of X-ray data reveals the formation of two conformers, with different degrees of distortions. The complex $[Mn(bpma)_2](ClO_4)_2$ promoted the H_2O_2 decomposition in good yields, and this characteristic inhibited the epoxidation of cyclohexene when this oxidant was used. Otherwise, when using PhIO as oxidant good yields of epoxidation (∼90%) were observed in homogeneous reactions. For heterogeneous catalysis the reactions were more selective for alcohol (∼70% yields).

Acknowledgements

The authors are grateful to Conselho Nacional de Desenvolvimento Científico e Tecnológico (CNPq), Coordenação de Aperfeiçoamento de Pessoal de Nível Superior (CAPES), Fundação Araucária, Fundação da Universidade Federal do Paraná (FUNPAR) and Universidade Federal do Paraná (UFPR) for the financial support. They gratefully acknowledge Msc. Geraldo R. Friedermann and Dr. Antonio S. Mangrich for the EPR facilities and analyses.

Appendix A. Supplementary data

Supplementary data associated with this article can be found, in the online version, at doi:10.1016/j.molcata.2006.12.044.

References

[1] K. Wieghardt, Angew. Chem. Int. Ed. Engl. 28 (1989) 1153–1172.
[2] D.P. Kessissoglou, Coord. Chem. Rev. 185/186 (1999) 837–858.
[3] J.H. Koek, E.W.M.J. Kohlen, S.W. Russell, L. van der Wolf, P.F. ter Steeg, J.C. Hellemons, Inorg. Chim. Acta 295 (1999) 189–199.
[4] M. Salavati-Niasari, F. Farzaneh, M. Ghandi, J. Mol. Catal. A: Chem. 186 (2002) 101–107.
[5] F. Farzaneh, M. Majidian, M. Ghandi, J. Mol. Catal. A: Chem. 148 (1999) 227–233.
[6] J. Brinksma, R. Hage, J. Kerschner, B.L. Feringa, Chem. Commun. (2000) 537–538.
[7] J. Brinksma, L. Schmieder, G. van Vliet, R. Boaron, R. Hage, D.E. De Vos, P.L. Alsters, B.L. Feringa, Tetrahedron Lett. 43 (2002) 2619–2622.
[8] C.R. Goldsmith, A.P. Cole, T.D.P. Stack, J. Am. Chem. Soc. 127 (2005) 9904–9912.
[9] P.-P. Knops-Gerrits, D.E. De Vos, P.A. Jacobs, J. Mol. Catal. A: Chem. 117 (1997) 57–70.
[10] M. Salavati-Niasari, F. Farzaneh, M. Ghandi, L. Turkian, J. Mol. Catal. A: Chem. 157 (2000) 183–188.
[11] B.C. Dave, R.S. Czermuszewicz, Inorg. Chim. Acta 281 (1998) 25–35.
[12] M. Mikuriya, H. Fukumoto, T. Kato, Inorg. Chem. Commun. 1 (1998) 225–227.
[13] I. Romero, L. Dubois, M.-N. Collomb, A. Deronzier, J.-M. Latour, J. Pécaut, Inorg. Chem. 41 (2002) 1795–1806.
[14] S.K. Mandal, W.H. Armstrong, Inorg. Chim. Acta 229 (1995) 261–270.
[15] D.P. Kessissoglou, W.M. Butler, V. Pecoraro, J. Chem. Soc., Chem. Commun. 16 (1986) 1253–1255.
[16] D.W. Gruenwedel, Inorg. Chem. 7 (1968) 495–501.
[17] Enraf-Nonius, CAD-4 EXPRESS. Version 5.1/1.2, Enraf-Nonius, Delft, The Netherlands, 1994.
[18] A.C.T. North, D.C. Phillips, F.S. Mathews, Acta Crystallogr. Sect. A 24 (1968) 351–359.
[19] A.L. Spek, PLATON, A Multipurpose Crystallographic Tool, Utrecht University, Utrecht, The Netherlands, 2006.
[20] Altomare, M.C. Burla, M. Camalli, G.L. Cascarano, C. Giacovazzo, A. Guagliardi, A.G.G. Moliterni, G. Polidori, R. Spagna, J. Appl. Cryst. 32 (1999) 115–119.
[21] SHELXL-97.
[22] L.J. Farrugia, J. Appl. Cryst. 32 (1999) 837–838.
[23] V.V. Barynin, M.M. Whittaker, S.V. Antonyuk, V.S. Lamzin, P.H. Harrison, P.J. Artymiuk, J.W. Whittaker, Structure 9 (2001) 725–738.
[24] B. Mabad, P. Cassoux, J.-P. Tuchagues, D.N. Hendrickson, Inorg. Chem. 25 (1986) 1420–1431.
[25] J.-J. Zhang, Y.-Y. Tang, Q.-H. Luo, C.-Y. Duan, Z.-L. Wang, Y.-H. Mei, Polyhedron 20 (2001) 2285–2291.
[26] M. Itoh, K.-I. Motoda, K. Shindo, T. Kamiusuki, H. Sakiyama, N. Matsumoto, H. Okawa, J. Chem. Soc., Dalton Trans. (1995) 3635–3641.
[27] R. Krishnan, S. Vancheesan, J. Mol. Catal. A: Chem. 142 (1999) 377–382.
[28] T. Nakamura, K. Niwa, S. Usugi, H. Asada, M. Fujiwara, T. Matsushita, Polyhedron 20 (2001) 191–201.
[29] V.L. Pecoraro, M.J. Baldwin, A. Gelasco, Chem. Rev. 94 (1994) 807–826.
[30] A.J. Wu, J.E. Penner-Hahn, V.L. Pecoraro, Chem. Rev. 104 (2004) 903–938.
[31] B. Mabad, P. Cassoux, J.-P. Tuchages, D.N. Hendrickson, Inorg. Chem. 25 (1986) 1420–1431.
[32] Y. Naruta, K. Maruyama, J. Am. Chem. Soc. 113 (1991) 3595–3596.
[33] Y. Naruta, M. Sasayama, T. Sasaki, Angew. Chem. Int. Ed. Engl. 33 (1994) 1839–1841.
[34] J. Haber, J. Iwanejko, P. Battioni, R. Mansuy, J. Mol. Catal. A: Chem. 152 (2000) 111–115.
[35] G. Simonneaux, P. Tagliatesta, J. Porph. Phtaloc. 8 (2004) 1166–1171.

[36] A.J. Appleton, S. Evans, J.R. Lindsay Smith, J. Chem. Soc., Perkin Trans. 2 (1995) 281–285.
[37] C.A. Sureshan, P.K. Bhattacharya, J. Mol. Catal. A: Chem. 136 (1998) 285–291.
[38] A.R. Silva, J. Vital, J.L. Figueiredo, C. Freire, B. Castro, New J. Chem. 27 (2003) 1511–1517.
[39] X.-D. Du, X.-D. Yu, J. Mol. Catal. A: Chem. 126 (1997) 109–1131.
[40] J.T. Groves, D.V. Subramanian, J. Am. Chem. Soc. 106 (1984) 2177–2181.
[41] E. Nascimento, G.F. Silva, F.A. Caetano, M.A.M. Fernandes, D.C. da Silva, M.E.M.D. de Carvalho, J.M. Pernaut, J.S. Rebouças, Y.M. Idemori, J. Inorg. Biochem. 99 (2005) 1193–1204.